NATIONAL ADVISORY COMMITTEE FOR AERONAUTICS

TECHNICAL NOTE 3399

A RAPID APPROXIMATE METHOD FOR THE DESIGN OF HUB SHROUD PROFILES OF CENTRIFUGAL IMPELLERS OF GIVEN BLADE SHAPE

By Kenneth J. Smith and Joseph T. Hamrick

Lewis Flight Propulsion Laboratory
Cleveland, Ohio

Washington
March 1955

NATIONAL ADVISORY COMMITTEE FOR AERONAUTICS

TECHNICAL NOTE 3399

A RAPID APPROXIMATE METHOD FOR THE DESIGN OF HUB SHROUD PROFILES OF CENTRIFUGAL IMPELLERS OF GIVEN BLADE SHAPE

By Kenneth J. Smith and Joseph T. Hamrick

SUMMARY

A rapid approximate method for the design of centrifugal compressors of given blade shape with compressible nonviscous flow characteristics has been developed using techniques based upon stream-filament theory. Axial symmetry is assumed, but meridional-plane forces derived from tangential pressure gradients are included.

The method was applied to the design of an impeller in order to determine the approximate maximum meridional streamline spacing that could be used. Three numerical solutions for different streamline spacings were made using the same hub profile, blade shape, and prescribed velocity distribution along the hub. The shroud profiles obtained from the three solutions, which utilized 3, 5, and 9 streamtubes, were negligibly different. The approximate computing time required was 15 hours per streamtube.

INTRODUCTION

The complex nature of flow within centrifugal compressors makes exact design of compressor components difficult. Methods in which an exact three-dimensional approach has been used are of necessity long and tedious processes (e.g., ref. 1). This tedium has led to the development of many approximate methods, in which a two-dimensional or a quasi-three-dimensional attack has been employed (see e.g., ref. 2). These methods are less time consuming and quite satisfactory for engineering purposes. The design method presented in this report is intended to speed the process still further and also to present a visualization of the mechanics of the fluid flow in the meridional plane while the design progresses.

The design method was developed at the NACA Lewis laboratory, using as a basis stream-filament methods, reported in reference 3, for analyzing flow through a centrifugal compressor. Since the design and the analysis solutions are merely inverses of each other, limitations and assumptions pertaining to the analysis method also apply to the design method. Thus, the design solution is adequate only so long as the assumption of axial symmetry can be used.

The method developed was applied to the design of an impeller having given hub and blade shapes in order to determine the approximate maximum meridional streamline spacing that can be used in the calculations with acceptable results. Three numerical solutions employing varied streamline spacings were made using the same combination of hub profile, blade shape, and prescribed velocity distribution along the hub. 3509

DEVELOPMENT OF DESIGN METHOD

For the flow-analysis method given in reference 3, a complete geometrical description of the impeller including hub, shroud, and blade shapes was needed for a solution. The design method applies the techniques of the flow-analysis method to obtain a shroud shape starting from a given blade shape, hub shape, and hub velocity distribution. The equations developed in the analysis solution apply equally well to the design method.

Outline of method. - From elementary streamline-flow theory, a series of annular concentric streamtubes are computed in sequence; the end point of the sequence is reached when the summation of the streamtube flows equals the desired over-all weight flow. The manner in which this is accomplished is as follows:

(1) A blade shape, a hub shape, and an average velocity distribution least conducive to boundary layer build-up are chosen.

(2) A meridional-plane hub profile is drawn and several stations between the impeller inlet and outlet are established.

(3) An estimated streamline is drawn forming a streamtube adjacent to the hub.

(4) The velocity at each intersection of the streamline with a normal from a hub station is computed from the assumed hub velocity distribution and the velocity equation derived in reference 3.

(5) The weight flow past each normal, based on flow conditions at the midline of the streamtube, is then computed to check for continuity of flow through the streamtube.

If continuity has not been established, the streamline spacing is adjusted and the procedure repeated until the weight flows at the several stations match. This final streamline becomes the new base streamline; its velocity distribution is given by the final values of the computations. An adjacent streamtube is constructed and the method repeated. When enough streamtubes have been constructed to carry the over-all weight flow desired, the final streamline determines the shape of the impeller shroud.

Assumptions. - The flow is assumed to be isentropic, steady, compressible, and nonviscous. Axial symmetry is assumed, but forces in the meridional plane that are derived from tangential pressure gradients are accounted for in the development of the flow equations (ref. 3). The average angle of flow relative to the meridional plane is taken equal to the blade angle β. This assumption is valid except at inlet for weight flows not in the vicinity of that required for zero angle of attack. At outlet, β must be modified to allow for slip, especially in computing the blade-to-blade velocity distribution.

Geometry. - Complete geometrical descriptions of the blade plan and of the hub shape of the impeller are needed for a numerical solution. The symbols denoting the geometrical quantities and their relation to the design method are given in appendix A and figure 1, respectively. The design method does not require the starting profile to be the hub shape, but an intermediate streamline or the shroud shape could be specified instead. Experience thus far has shown, however, that it is best to start in a region in which velocity changes have the greatest effect on streamline spacing. Such a region is generally found near the hub, where there is low weight flow per unit area, and blade blockage is greatest.

Velocity equation. - A force equation was obtained in reference 3 by summing the forces acting on a particle moving along the streamline path. The force equation, when combined with a form of the general energy equation, resulted in an equation involving the relative velocity q and a number of geometric variables. The general velocity equation obtained was then simplified for the case of radial blade elements and no prerotation to

$$\frac{dq}{dn} = aq - b \tag{1}$$

where a and b are parameters such that

$$a = \frac{\cos^2\beta}{r_c} - \frac{\sin^2\beta}{r \cos \alpha}$$

and

$$b = \frac{\sin \beta}{\cos \alpha}\left(\sin \alpha \cos \alpha \frac{du}{dz} + 2\omega\right)$$

3509 CI-1 back

When equation (1) was solved for the velocity q,

$$q = e^{\int_0^n a\,dn}\left(q_0 - \int_0^n b e^{-\int_0^n a\,dn}\,dn\right) \tag{2}$$

This equation relates the relative velocity at the hub to that at any other point along the path normal to the flow streamlines in the hub-to-shroud passages, for an impeller with radial blade elements and no prerotation. The general velocity equation is not considered in this report, since the trend of design has been toward radial blade elements and no prerotation; however, its use would introduce no limitations to the method beyond the added geometric complications.

3509

Equation (2) is applied to determine the velocity distribution along each streamline in the meridional plane, with the previous streamline as a base. An exact value of the equation would require integration; but because the intervals between streamlines are small, a good approximation to the exact value can be found when a and b are assumed constant and taken as average values between the two streamlines. The equation then simplifies to

$$q = q_0\,e^{a\Delta n} + b\left(\frac{1 - e^{a\Delta n}}{a}\right) \tag{3}$$

Continuity equation. - In reference 3, the equation for continuity of flow through the impeller was written

$$W = 2\pi \int_0^n r f \rho g q \cos\beta\,dn \tag{4}$$

For the design method, it is not necessary to establish flow across the complete passage, but only the increment of flow through the annulus between two adjacent stream surfaces. Flow conditions along the midline of the streamtube are considered and the equation becomes

$$w = 2\pi r f \rho g q \cos\beta\Delta n \tag{5}$$

The value of the density ρ, for no prerotation, is found from

$$\rho = \rho_{t,i}\left\{1 + \frac{\gamma - 1}{2}\left[\left(\frac{\omega r}{c_i}\right)^2 - \left(\frac{q}{c_i}\right)^2\right]\right\}^{\frac{1}{\gamma-1}} \tag{6}$$

EXAMPLE IMPELLER

The design operating conditions for the impeller were chosen as follows:

Equivalent impeller tip speed, $U/\sqrt{\theta}$, ft/sec 1331
Ratio of specific heats, γ 1.4
Prerotation 0

3509

The hub shape and the blade plan were those of the 18-blade mixed-flow centrifugal compressor described in reference 4. A detailed outline of the development of the shroud shape from the equations is given in appendix B together with the procedure used for the computations. Three solutions were calculated from the same hub shape, blade plan, and velocity distribution. The three, employing different numbers of streamlines, were calculated to note the effect of streamline spacing on the solution. A blade-to-blade analysis for the five-streamtube design was made to obtain the performance characteristics of the selected parabolic blade shape.

RESULTS AND DISCUSSION

Shroud profile. - Since total weight flow was the same for all three solutions, streamline spacing determined the number of streamtubes. The shroud coordinates obtained from three-, five-, and nine-streamtube designs are compared in table I. The tabulation shows the negligible effect on shroud shape produced by changing streamline spacing over this range. Visual errors, inherent in a method of this type, in determining the value of the coordinates and in making other graphical measurements account for minor deviations in the radius ratio. However, the maximum deviation between any two of the given radius ratios is less than 1/4 of 1 percent, with reference to the average radius ratio for the three solutions. Figure 2 shows the streamline pattern obtained from the spacing that resulted in five streamtubes.

Velocity ratio. - Lines of constant velocity ratio Q relative to the impeller, for the five-streamtube solution, are included in figure 2. Similar configurations were obtained for the other two solutions, with maximum differences among the three occurring at the shroud. The shroud velocity ratios obtained from the three-, five-, and nine-streamtube solutions are shown in table II. The deviations in the velocity ratios result from only slight differences in shroud coordinates. In the region of near-sonic velocity (Mach number, 0.9, e.g.), a change of 1 percent in flow area can produce a change of approximately 10 percent in velocity. The effect of area change on velocity is easily seen for the three-streamtube solution. However, since the deviations of the velocity distributions are comparable to those that would arise from area changes due to machining tolerances, any of the three distributions is acceptable for design purposes.

The specified velocity pattern along the hub, and the shroud velocity ratios calculated in the five-streamtube solution are shown in figure 3. The velocity distributions calculated in reference 3 for the original impeller have been included in the figure. The prescribed velocity pattern along the hub for the design method consists of a slowly decelerating flow for half the hub length, followed by a gradual acceleration for the remainder. With respect to avoiding boundary layer build-up and separation losses, this pattern is superior to the rapidly decelerating flow along most of the hub length as determined for the original impeller. The shroud velocity distribution of the new design is also better, for although the rate of deceleration is about the same as that of the original impeller, the length of path over which deceleration occurs is shorter. The most desirable velocity pattern would be one in which flow accelerated along the entire length of both hub and shroud. However, the shroud velocity distribution that accompanies a specified hub velocity distribution cannot, in general, be predicted. The sharp rise in velocity on the shroud is an example of the unpredictability that results from prescribing the velocity along any given path, particularly where large curvatures exist.

Blade surface velocities. - The meridional-plane relative velocity ratios for the streamlines and the midstreamtubes represent averages of those at the blade surfaces. To determine the surface velocities over the driving and the trailing faces of the blades, the method described in appendix D of reference 3 is applied. Velocity distributions over the blade surfaces for the several streamtubes of the five-streamtube solution are shown in figure 4. Although the flow decelerates rapidly along the driving face, separation should not occur there since experiments have shown that a boundary layer does not build up on the driving face. For all the streamtubes, the rate of deceleration along the trailing face is about equal to that at midpassage. From considerations of blade loading distribution, the combination of small difference in blade surface velocities upstream from L equal 0.35 and large difference thereafter is undesirable. A more uniform velocity ratio distribution could be obtained by changing blade shape or by introducing splitter vanes extending downstream from L equal 0.35. The introduction of these splitter vanes would also, by decreasing the loading per blade, reduce any tendency for an eddy to form on the driving face.

Calculations of distribution of relative velocity on the blade surfaces should take account of the slip factor μ. Consequently, the mean relative velocity values developed in the meridional-plane computations are not applicable for these calculations. Values of mean relative velocity that account for slip factor were computed by using flow angles obtained by the method presented in reference 5. The higher values so calculated were compared with the values previously calculated to determine the effect on streamline spacing. It was found that the product ρv remained approximately constant for the small increase in relative velocity (approximate average 6 percent at exit; see fig. 5), thus, streamline spacing was not changed significantly. However, the higher values of relative velocity calculated when the slip factor was considered had a large effect on blade loading near the exit. The results obtained from a blade-to-blade analysis that neglected slip factor indicated an eddy formation on the driving face. The eddy formation was not indicated when slip factor was considered because of the decreased loading. An indication of eddy flow is obtained when the solution yields a value of driving-face velocity that is imaginary or in the vicinity of zero. In either case, a higher velocity flow or more blades in the eddy region are needed.

Inlet angle of attack. - Theoretical determination of the exact hub-to-shroud variation of blade inlet angle required for most efficient operation is very difficult. The abrupt change in flow area at the inlet, the turning effect on the fluid, and velocity variation across the inlet annulus combine to make the solution of the problem arduous. The following approximate calculation of inlet flow angles relative to the blades provides a qualitative means of evaluating a particular blade inlet angle distribution. The net area of each streamtube (annulus area minus blade area) is computed and the through-flow velocity found from the designated weight flow for the streamtube. Vector addition of the through-flow velocity and the wheel speed at midstreamtube gives the approximate flow direction at inlet to the blades, with respect to the meridional plane. The approximate inlet angle relative to the blades is then the difference between this computed flow direction and the blade angle at midstreamtube. This computation of approximate angle of attack assumes that each streamtube extends upstream from the inlet and simulates a fixed annulus with no radial displacement of the streamlines from their calculated positions. In the actual case, there is a radial shift of the streamlines caused by the blade thickness taper from hub to shroud. A more nearly exact angle of attack may be derived by using values of the upstream flow angle and the deviation angle that take account of this radial shift of the streamlines (ref. 6). A comparison of the approximate angles of attack and the more nearly exact values is made in figure 6. The figure shows an average angle of attack of -2.5° for the more nearly exact solution, indicating an excessive weight flow at design conditions. The approximate solution shows a decreasing value of the angle of attack from hub to shroud due to the decreasing effect of blade blockage. Despite the disparity introduced by blockage effects, the approximate method of determining the angle of attack establishes whether the radial variation of inlet blade angle is approximately that required for efficient operation. It can be seen that the inlet blade angle variation for this impeller corresponded fairly well to the desired design conditions.

SUMMARY OF RESULTS

A rapid approximate method for the design of centrifugal compressors of given blade shape with compressible, nonviscous flow characteristics has been developed. It assumes axial symmetry, but includes meridional plane forces caused by tangential pressure gradients. The approximate computing time for a design is 15 hours per streamtube. The method was used, with streamline spacings that resulted in three, five, and nine streamtubes, for the design of an example impeller with blades of a parabolic shape. The following results were noted:

1. Large changes in streamline spacing had negligible effects on shroud shape. The accompanying variation in velocity distribution was in the range of that which would arise from machining tolerances.

2. Allowance for slip resulted in negligible changes in calculated shroud shape, but resulted in an exit relative velocity approximately 6 percent above that for the solution in which slip was neglected.

3. The parabolic blade shape produced an uneven loading distribution, with the major portion of the load occurring near the exit.

4. The inlet blade angles of this impeller were approximately those required for high efficiency at the design weight flow.

Lewis Flight Propulsion Laboratory
National Advisory Committee for Aeronautics
Cleveland, Ohio, December 6, 1954

3509

3509

CI-2

APPENDIX A

SYMBOLS

The following symbols are used in this report:

a	geometric parameter, $\frac{\cos^2\beta}{r_c} - \frac{\sin^2\beta}{r \cos \alpha}$
b	geometric parameter, $\frac{\sin \beta}{\cos \alpha}\left(2\omega + \sin \alpha \cos \alpha \frac{du}{dz}\right)$
c	stagnation speed of sound, ft/sec
f	blade blockage factor, $\frac{2\pi r - Nt}{2\pi r}$
g	gravitational acceleration, ft/sec^2
L	percent of total streamline length, from impeller inlet
N	number of blades
n	distance along normal from hub
Δn	distance between adjacent streamlines along normal, ft
P	fluid particle
Q	velocity ratio, q/c_i
q	velocity relative to impeller (fig. 1(c)), ft/sec
R	radius ratio, r/impeller tip radius
r	radius from axis of rotation to point being considered, ft
r_c	radius of curvature of streamlines in meridional plane (positive when streamline is concave upward), ft
r_h	hub radius
r'	slope of streamlines in meridional plane with respect to axis of rotation

r''	rate of change in slope r'
t	blade thickness at a given radius, ft
U	actual impeller tip speed, ft/sec
u	tangential velocity relative to impeller (positive in direction of rotation (fig. 1(c)), ft/sec
v	through-flow component of velocity (fig. 1(c)), ft/sec
W	total compressor flow ratio, lb/sec
w	incremental flow rate, lb/sec
z	axial distance from front of impeller hub, ft
α	angle between tangent to streamline in meridional plane and impeller axis of rotation, deg
β	blade angle (fig. 1(c), negative for backward-curved blades), deg
θ	ratio of inlet stagnation temperature to standard sea-level temperature
γ	ratio of specific heats
μ	slip factor, average absolute tangential velocity of fluid at impeller tip divided by impeller tip speed
ρ	mass density, lb-sec^2/ft^4
ρ_t	total mass density, lb-sec^2/ft^4
φ	blade angle in axial-tengential direction (fig. 1(b), negative for backward-curved blades), deg
ω	angular velocity of impeller, radians/sec

Subscripts:

i	inlet conditions
0,1,. . .	succeeding stations along streamlines

Superscripts:

-	values taken at midstreamtube

3509

3509 CI-2 back

APPENDIX B

NUMERICAL PROCEDURE

The meridional plane profile of the specified hub shape is drawn and a velocity distribution chosen. Normals to the hub profile are erected at various stations. Columns 1 to 7 and 9 to 12 (table III) are recorded for each station along the hub profile. It is emphasized that column 8 was used to find the blade angle β and applies only to the particular blade shape of this impeller. The equation for the blade curvature in the axial tangential plane (plane tangent to circular cylinder of radius r) is given by $\tan \varphi$ equals $1.3572 (12z - 3.93) r$, where z and r are in feet. Care must be taken to maintain the proper sign convention for the blade angles and the velocity components (see figs. 1(b) and (c)). A satisfactory approximation to the value of du/dz at each station along the midstreamtube can be found by plotting u against z from computations along the previous streamline. The value of the slope is recorded in column 13 and column 14 computed. These values remain constant throughout the iterative process which follows.

Geometry. - Columns 16 to 24 and column 37 are concerned with the basic geometry. The spacing of the first streamline along each normal to the hub profile is estimated and the chosen value recorded in column 15. Half of the value of column 15 is laid off along its corresponding normal to define the midline of the streamtube. Columns 16, 17, and 18 are recorded for each station along the midline of the streamtube. Column 17 is equal to the hub radius at the $\bar{z}$ value of column 18 (see fig. 1(a)), and is used in the determination of blade thickness at the midline. (The blade for this impeller has a constant thickness of 0.210 inch at the hub with a 3° taper in the radial direction.) The radius of curvature at each station along the midline (column 19) is found from $r_c = \left[1 + (r')^2\right]^{3/2} / r''$ or, as was done in this report, by mechanical means (ref. 7). Column 37, equivalent to $2\pi r - Nt$, is the net circumferential length at each station along the midline. The constants used in column 37 will apply only to this blade shape. Attention is called to the fact that the value of the symbol f in equation (5) is not calculated directly, since f is equivalent to $1 - Nt/2\pi r$. Experience has shown the angle α is essentially the same for streamline and midline, hence the value of column 3 is used for α of the midline. Columns 22 to 24 complete the blade geometry needed for further computations. It is again noted that column 21 applies only to the blade shape of this impeller.

Velocity. - Columns 25 to 30 apply to the computation of the velocity given by equation (3) in the text. The combination of terms in each column are readily compared with the equation and are explained in the column headings. Column 31 gives the value of the velocity at the intersection of the estimated streamline and each normal. Since a linear variation of velocity between streamlines is assumed, the velocity at the midline of the streamtube (column 32) is simply the average of column 31 and column 7.

Density equation. - Equation (6) for the density $\bar{\rho}$ includes a number of constants that have been combined in columns 33 and 34 for more rapid calculation. As can be noted from equation (6), the numerical value of the combination will vary with the specified operating conditions for the impeller. The value arrived at in column 36 is equal to the dimensionless ratio $\bar{\rho}/\rho_{t,i}$, the exact value of $\bar{\rho}$ not being required for finding the streamline spacing. 3509

Continuity equation. - The continuity equation as given by equation (5) is $w = 2\pi r f \rho g q \cos \beta \, \Delta n$. Equating the average weight flows across each normal yields $(2\pi r f \rho q \cos \beta \, \Delta n)_1 = (2\pi r f \rho q \cos \beta \, \Delta n)_2 = \ldots (2\pi r f \rho q \cos \beta \, \Delta n)_n$. Then $\Delta n_{1,2} = (2\pi r f \rho q \cos \beta \, \Delta n)_n / (2\pi r f \rho q \cos \beta)_{1,2}$ where subscript n refers to values at any designated station along the midline. This procedure is carried out in columns 38 and 39. The weight flow for the chosen reference station, hence for the streamtube, is the product of $\rho_{t,i}$, g, column 38, and column 39. The values obtained in column 39 for each station are compared with the original estimates in column 15. Should the values of columns 39 and 15 not coincide within the specified limits, the streamline spacing is revised, using the computed values of column 39 as the next estimate for column 15, and the procedure repeated. In the example problem, convergence was achieved within three significant figures by the second iteration. After a satisfactory convergence between columns 15 and 39 has been reached, the final values of column 39 are marked on the solution and the streamline drawn. This streamline becomes the new base streamline. Normals to the new base streamline are constructed from each station along the midline of the previous streamtube in order to obtain a line more nearly normal to all streamlines. The velocity at each station along the new base streamline (column 7) is given by the final computations recorded in column 31. The sequence of operations is repeated, using the final values of column 39 as estimates for column 15 of the succeeding streamline, until enough streamtubes have been formed to carry the desired weight flow. The approximate time required to compute and check the three solutions made in this report was 15 hours for each streamtube.

REFERENCES

1. Wu, Chung-Hua: A General Theory of Three-Dimensional Flow in Subsonic and Supersonic Turbomachines of Axial-, Radial-, and Mixed-Flow Types. NACA TN 2604, 1952.

2. Stanitz, John D.: Approximate Design Method for High-Solidity Blade Elements in Compressors and Turbines. NACA TN 2408, 1951.

3. Hamrick, Joseph T., Ginsburg, Ambrose, and Osborn, Walter M.: Method of Analysis for Compressible Flow Through Mixed-Flow Centrifugal Impellers of Arbitrary Design. NACA Rep. 1082, 1952. (Supersedes NACA TN 2165.)

4. Anderson, Robert J., Ritter, William K., and Dildine, Dean M.: An Investigation of the Effect of Blade Curvature on Centrifugal-Impeller Performance. NACA TN 1313, 1947.

5. Stanitz, John D., and Prian, Vasily D.: A Rapid Approximate Method for Determining Velocity Distribution on Impeller Blades of Centrifugal Compressors. NACA TN 2421, 1951.

6. Stanitz, John D.: Effect of Blade-Thickness Taper on Axial-Velocity Distribution at the Leading Edge of an Entrance Rotor-Blade Row with Axial Inlet, and the Influence of This Distribution on Alinement of the Rotor Blade for Zero Angle of Attack. NACA TN 2986, 1953.

7. Stewart, Warner L.: Analytical Investigation of Flow Through High-Speed Mixed-Flow Turbine. NACA RM E51H06, 1951.

TABLE I. - SHROUD COORDINATES FOR THREE-, FIVE-, AND NINE-STREAMTUBE SOLUTIONS $\left(R = \frac{r}{\text{impeller tip radius}}\right)$

z, ft	R		
	Number of streamtubes		
	3	5	9
0.0092	0.6666	0.6666	0.6666
.0290	.6702	.6710	.6710
.0580	.6794	.6794	.6796
.0870	.6890	.6882	.6890
.1160	.6962	.6964	.6970
.1450	.7082	.7088	.7090
.1740	.7292	.7296	.7290
.2030	.7614	.7616	.7608
.2320	.8102	.8090	.8094
.2610	.8820	.8800	.8818
.2900	.9954	.9952	.9952

3509

TABLE II. - SHROUD VELOCITY RATIO DISTRIBUTIONS FOR THREE-, FIVE-, AND NINE-STREAMTUBE SOLUTIONS

z, ft	Velocity ratio, Q		
	Number of streamtubes		
	3	5	9
0.0092	0.981	0.983	0.986
.0290	1.000	.977	.979
.0580	.930	.938	.939
.0870	.888	.900	.900
.1160	.968	.976	.956
.1450	.979	.977	.960
.1740	.960	.948	.945
.2030	.908	.910	.899
.2320	.825	.840	.817
.2610	.730	.744	.725
.2900	.647	.648	.645

TABLE III. - STREAMLINE CALCULATION PROCEDURE

Station	1	2	3	4	5	6	7	8	9	10	11	12
				sin 3	cos 3	4 5	31 Previous stream-line	16.286 × 1 -5.334	2 ×5 ×8	$\tan^{-1}$ 9	sin 10	× 7 11
	z	r	α	sin α	cos α	sin α cos α	q	K	tan β	β	sin β	u
0	0.0000	0.0000	0.00	0.0000	0.0000	0.0000	0	0.000	0.0000	0.00	0.0000	0
1												
2												
3												

Station	13	14	15	16	17	18	19	20	21	22	23
	From plot 12 vs. 1	$\frac{[6\ 13\ +2\omega]}{5}$						5 16	16.286 × 18 -5.334	20 21	sin $[\tan^{-1}$ 22$]$
	du/dz		Δn	$\bar{r}$	$\bar{r}_h$	$\bar{z}$	$\bar{r}_c$	$\bar{r}$ cos α	$\bar{K}$	tan $\bar{\beta}$	sin $\bar{\beta}$
0	0	0	0.00000	0.0000	0.0000	0.0000	0.000	0.0000	0.000	0.0000	0.0000
1											
2											
3											

Station	24	25	26	27	28	29	30	31	32
	cos $[\tan^{-1}$ 22$]$	$\frac{24^2}{19}$	$\frac{23^2}{20}$	[25 - 26]	$e^{15\ 27}$	$\frac{1.0-28}{27}$	14 23	[7 28] + [29 30]	$\frac{[7+31]}{2.0}$
	cos $\bar{\beta}$	$\frac{\cos^2\bar{\beta}}{\bar{r}_c}$	$\frac{\sin^2\bar{\beta}}{\bar{r}\cos\alpha}$	a	$e^{a\Delta n}$	$\frac{1-e^{a\Delta n}}{a}$	b	q	$\bar{q}$
0	0.0000	0.000	0.000	0.0000	0.0000	0.00000	0	0	0
1									
2									
3									

TABLE III. - Concluded. STREAMLINE CALCULATION PROCEDURE

Station	33	34	35	36	37	38	39
	$1.606\times10^{-7}\times(32)^2$	$1.138\times(16)^2$	$(34)-(33)+1.0$	$(35)^{2.5}$	$7.226\,(16)-.943\,(17)-.315$	$(24)\times(32)\times(36)\times(37)$	$\frac{(15)_n\;(38)_n}{(38)}$
				$\frac{\bar{\rho}}{\rho_{t,i}}$	$2\pi r-Nt$		Δn
0	0.0000	0.0000	0.0000	0.0000	0.000	0	0.00000
1							
2							
3							

3509

3509

CI-3

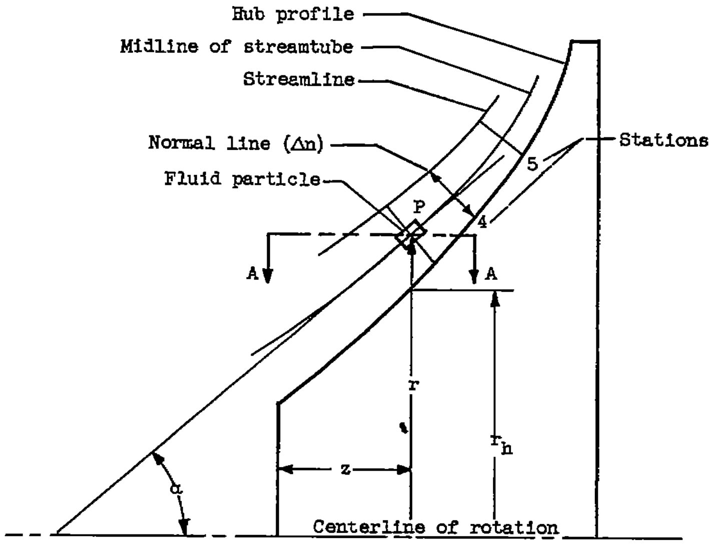

(a) Meridional plane configuration.

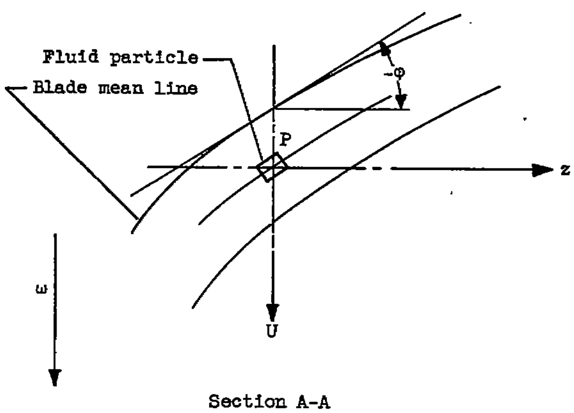

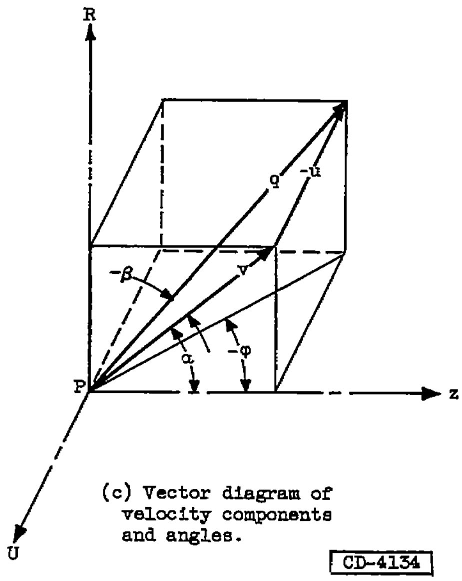

(c) Vector diagram of velocity components and angles.

(b) Location of φ on developed cylindrical surface.

Figure 1. - Impeller geometry used in development of design method.

3509

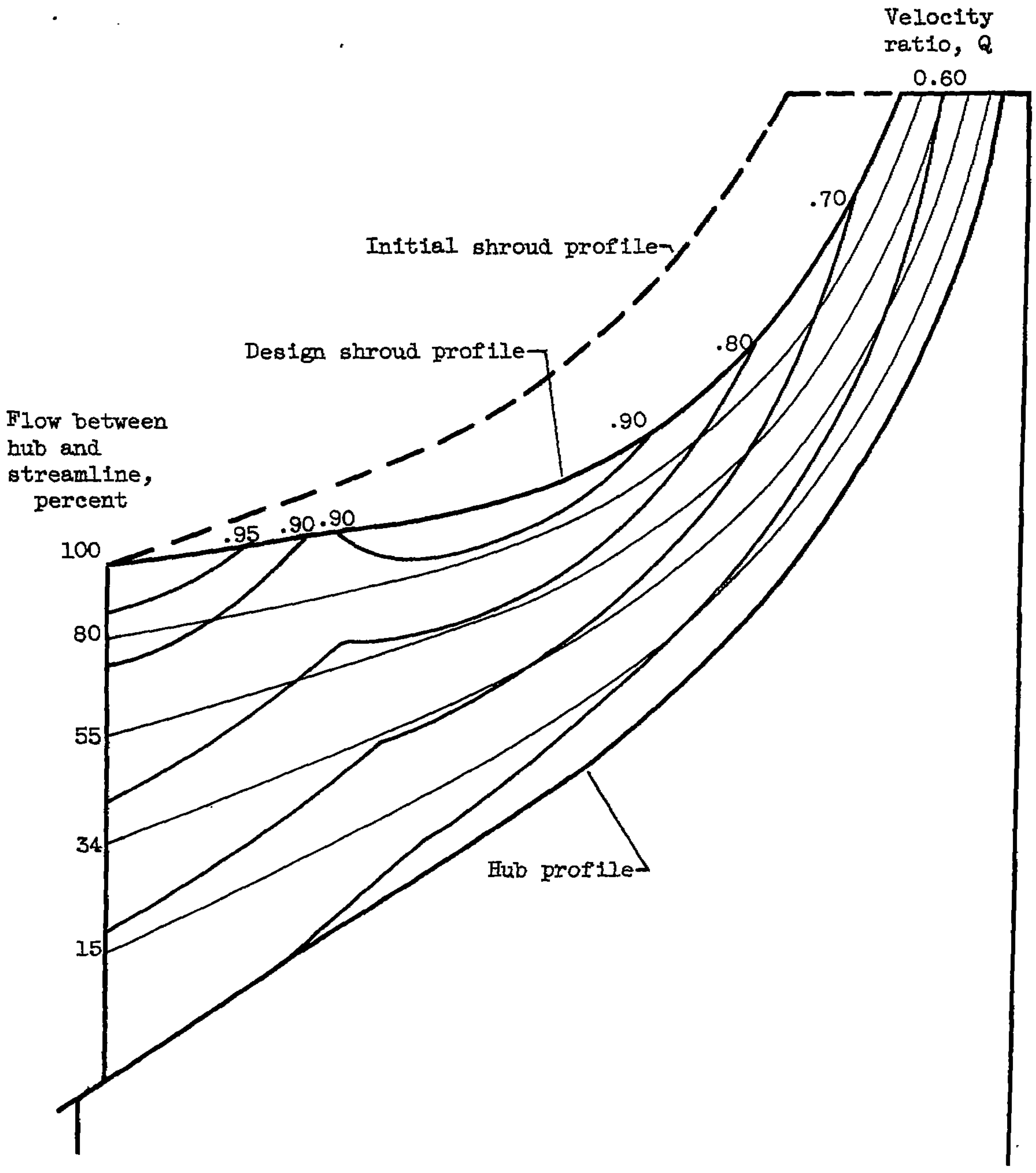

Figure 2. - Flow analysis in meridional plane for five-streamtube solution.

3509

CI-3 back

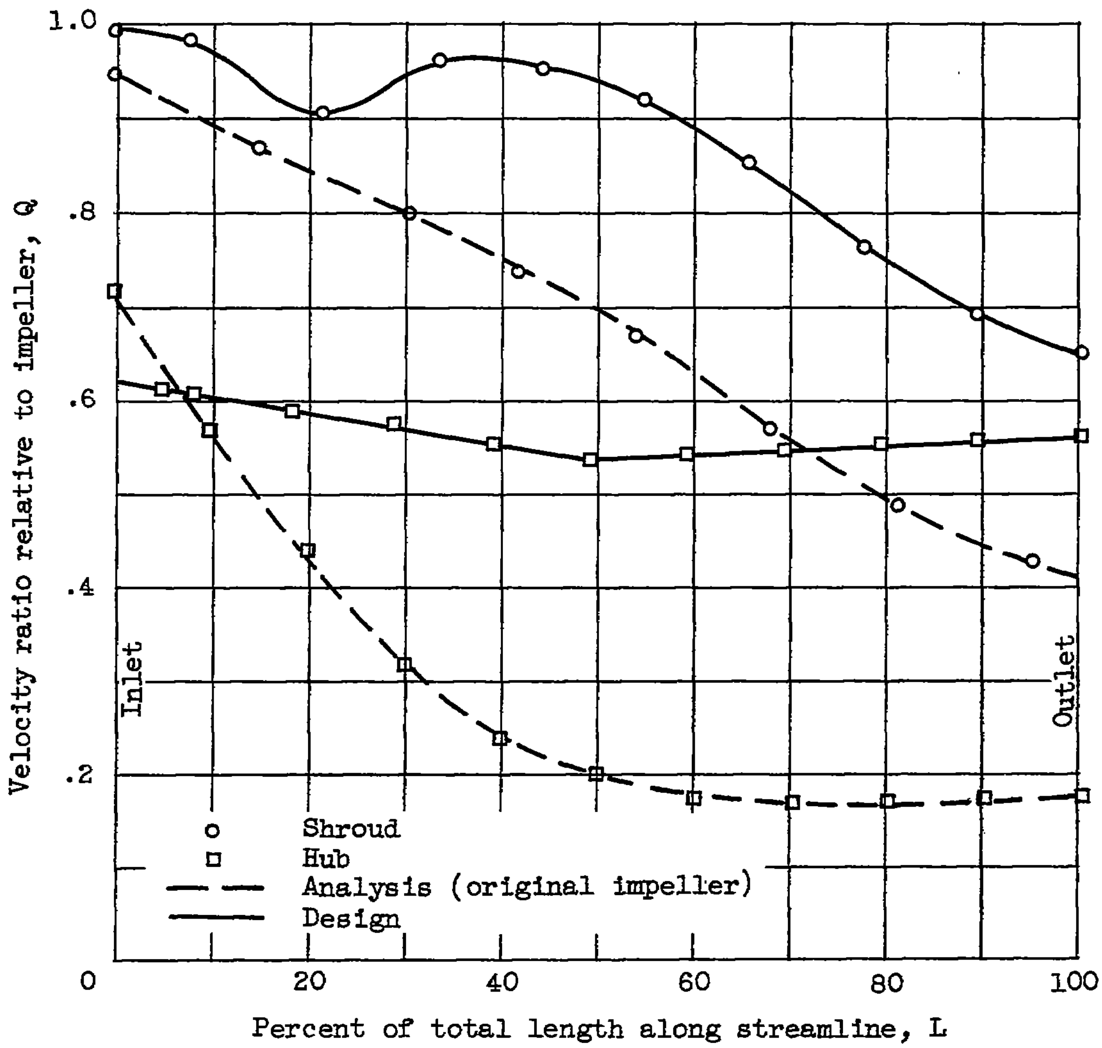

Figure 3. - Comparison of design hub and shroud velocity distributions with results from analysis of original impeller; slip factor neglected.

3509

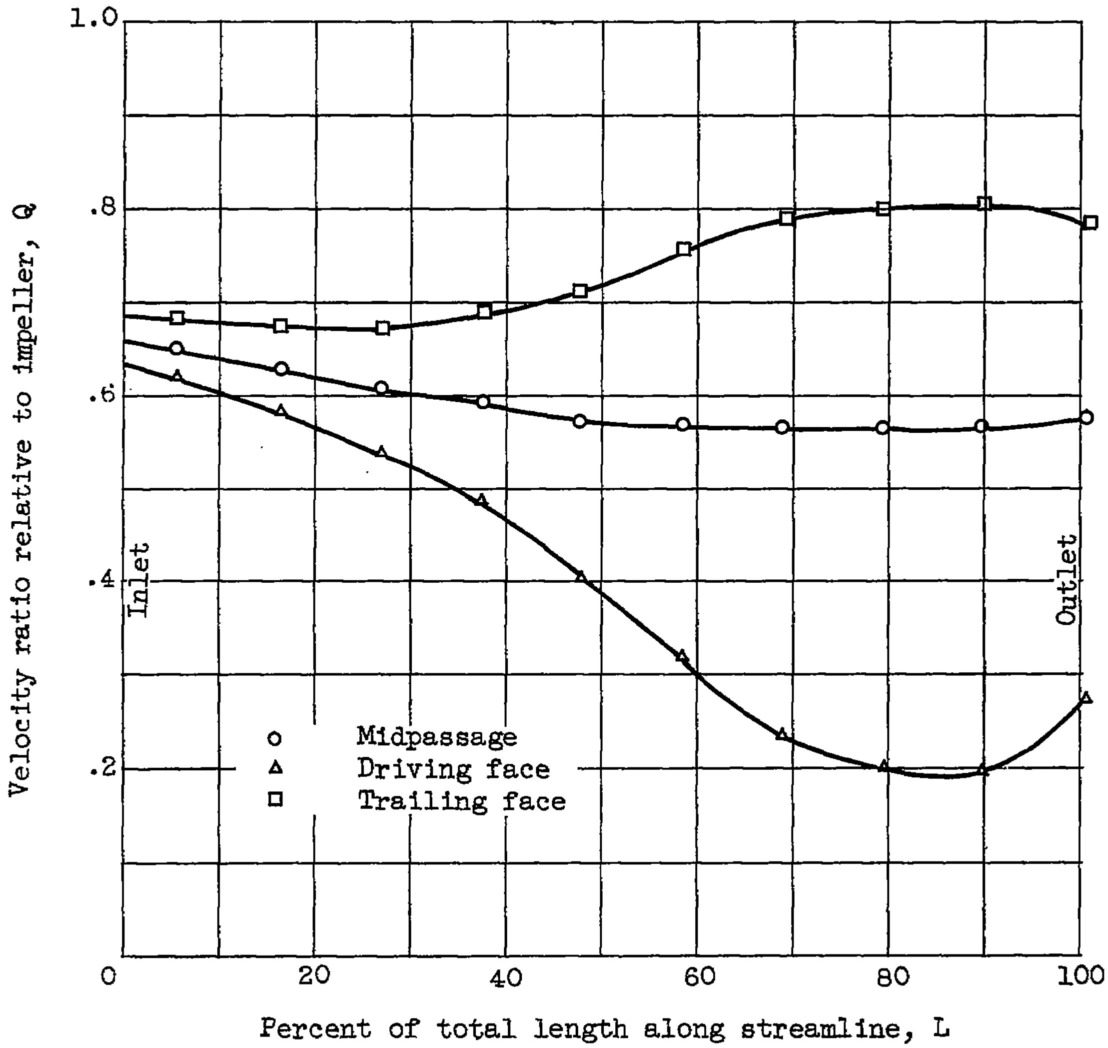

(a) Streamtube 1.

Figure 4. - Blade surface velocity ratios for the five-streamtube solution including slip factor (μ = 0.89).

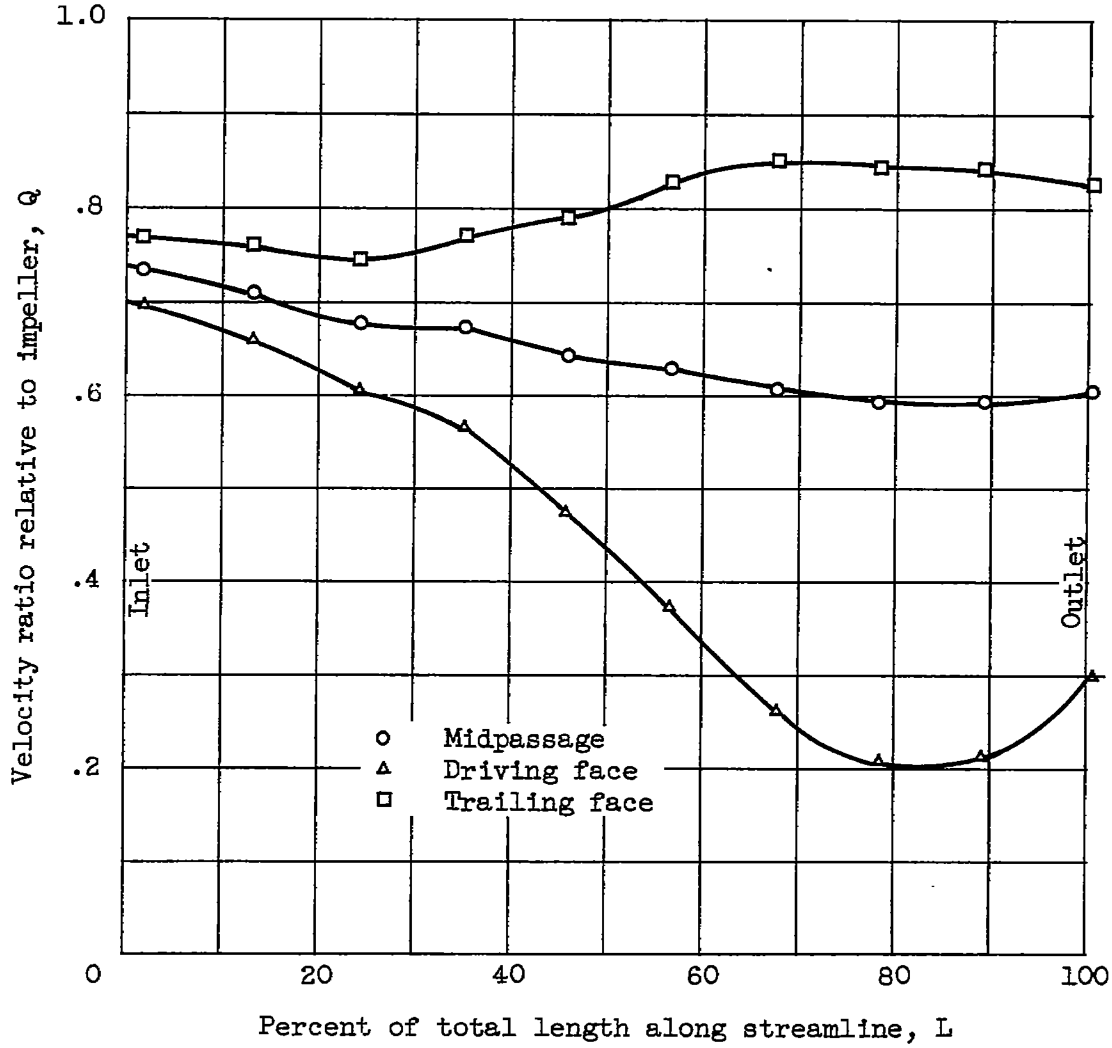

(b) Streamtube 2.

Figure 4. - Continued. Blade surface velocity ratios for the five-streamtube solution including slip factor (μ = 0.89).

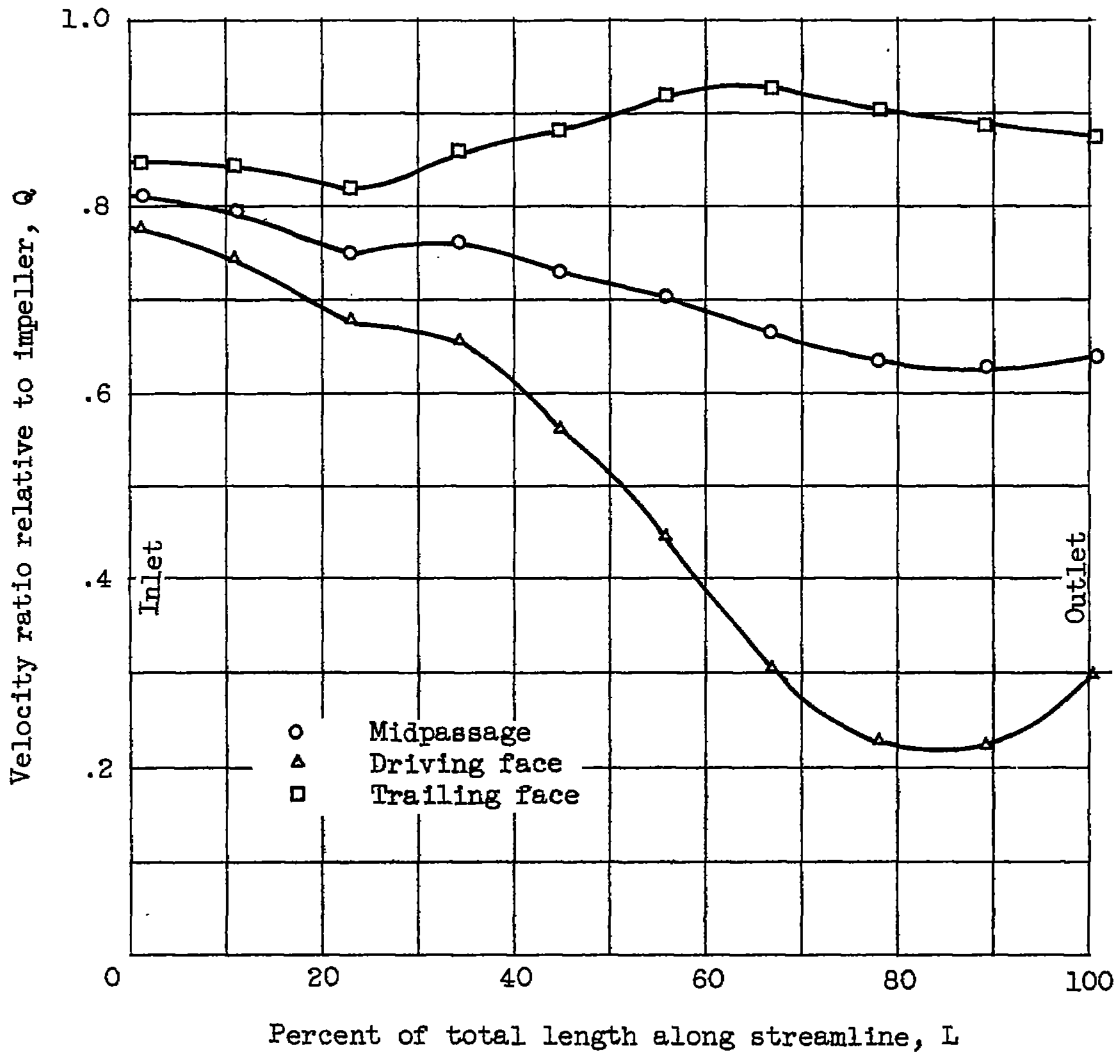

(c) Streamtube 3.

Figure 4. - Continued. Blade surface velocity ratios for the five-streamtube solution including slip factor (μ = 0.89).

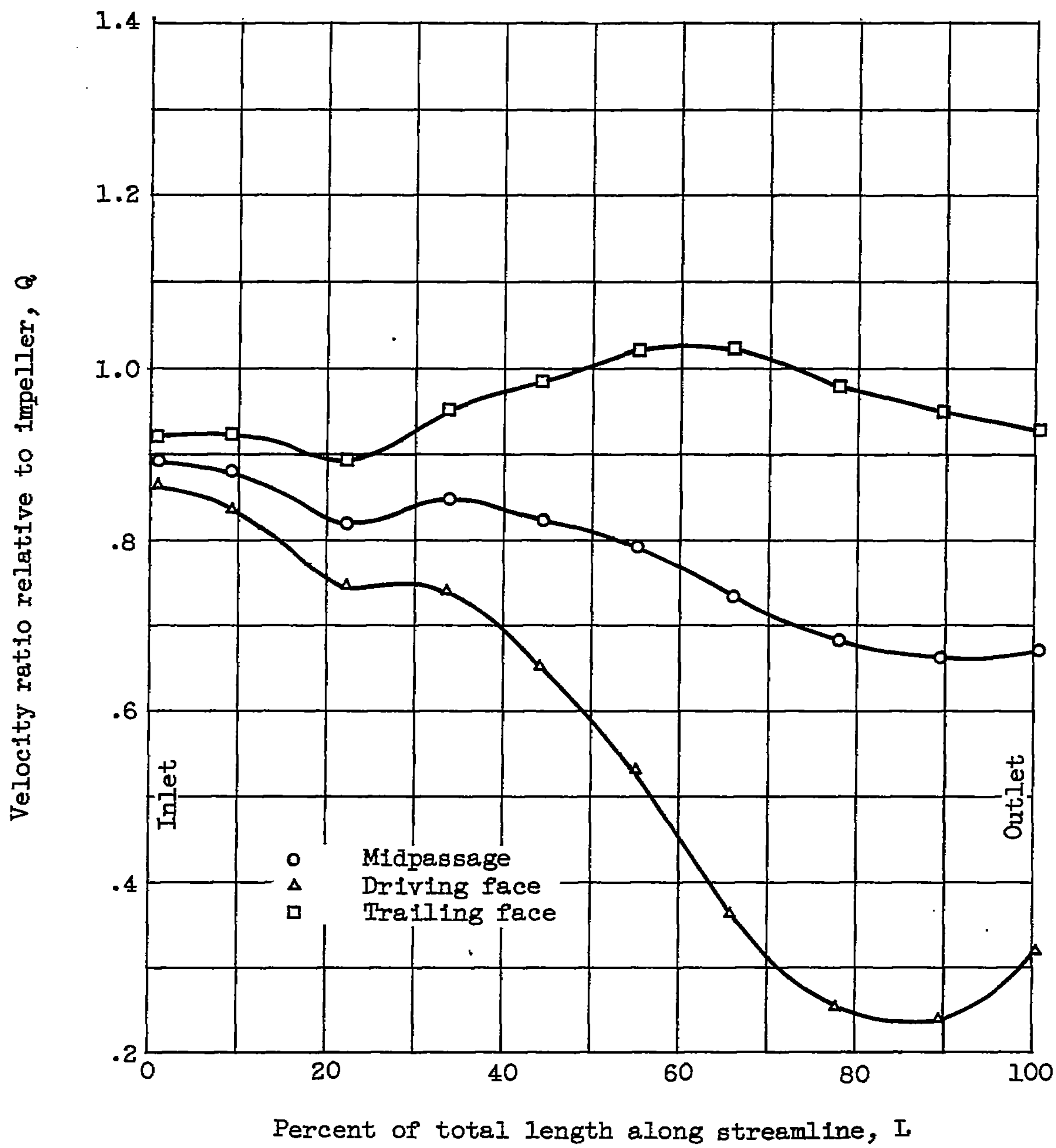

(d) Streamtube 4.

Figure 4. - Continued. Blade surface velocity ratios for the five-streamtube solution including slip factor (μ = 0.89).

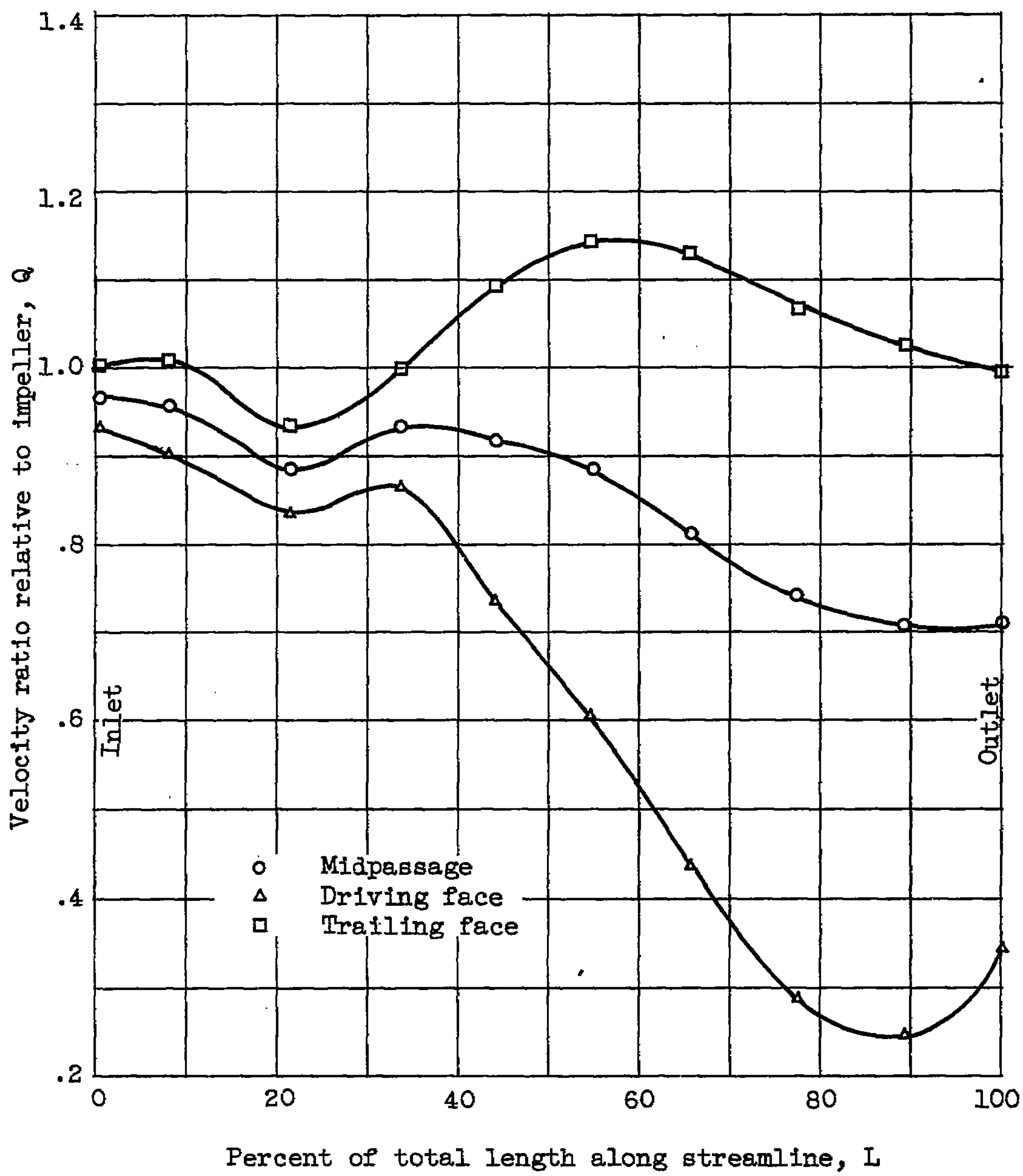

(e) Streamtube 5.

Figure 4. - Concluded. Blade surface velocity ratios for the five-streamtube solution including slip factor ($\mu = 0.89$).

3509

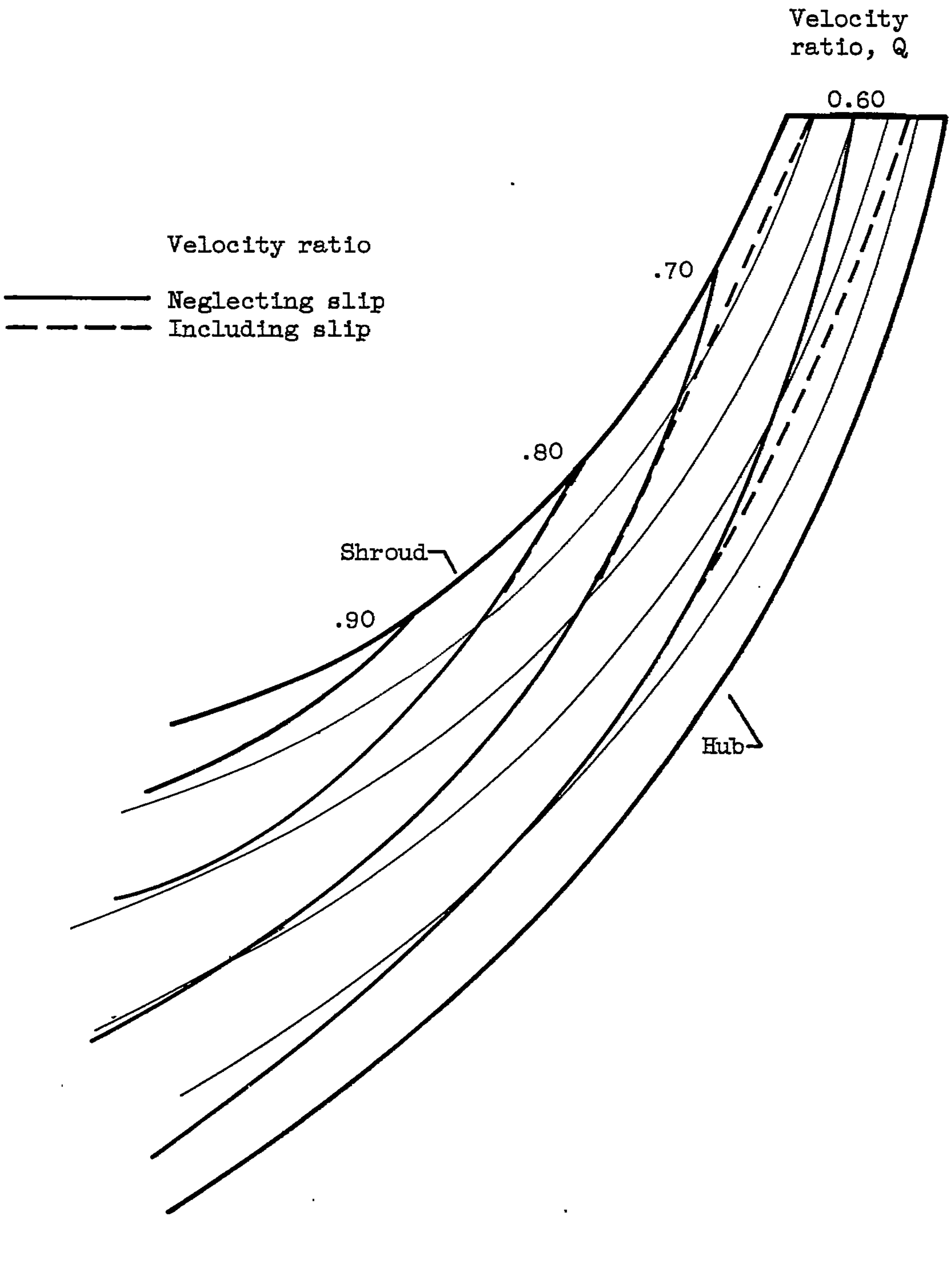

Figure 5. - Effect of slip factor ($\mu = 0.89$) on velocity ratios in meridional plane for five-streamtube solution.

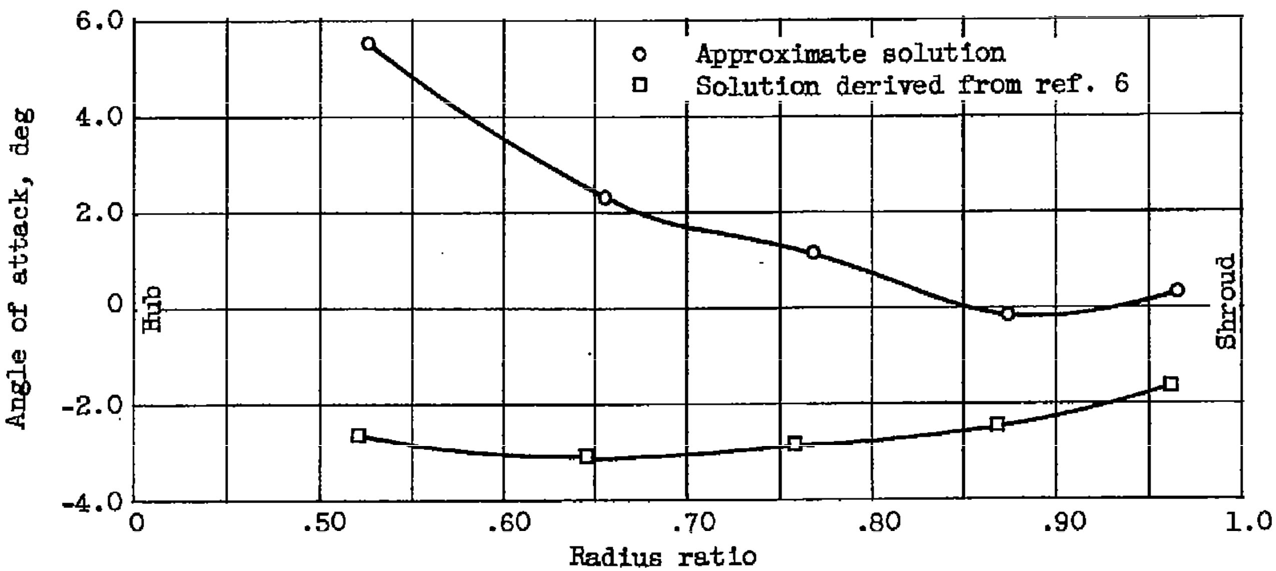

Figure 6. - Angles of attack calculated with (ref. 6) and without (approximate solution) consideration of radial displacement of streamlines ahead of impeller.